Respiratory Physiology & Neurobiology 219 (2015) 85–94

Contents lists available at ScienceDirect

Respiratory Physiology & Neurobiology

journal homepage: www.elsevier.com/locate/resphysiol

Chronic hypoxia and hyperoxia modifies morphology and VEGF concentration of the lungs of the developing chicken (*Gallus gallus* variant *domesticus*)

Melissa A. Lewallen, Warren W. Burggren*

Developmental and Integrative Biology Research Group, Department of Biological Sciences, University of North Texas, 1155 Union Circle #305220, Denton, TX 76203, USA

ARTICLE INFO

Article history:
Received 22 December 2014
Received in revised form 11 August 2015
Accepted 17 August 2015
Available online 20 August 2015

Keywords:
Hypoxia
Hyperoxia
VEGF
Lung morphology
Chicken embryo
Parabronchi

ABSTRACT

Embryo body and lung wet and dry mass, pulmonary morphometrics and pulmonary VEGF concentrations were determined in developing chicken embryos at days 16 and 18 (D16, D18) in three populations: incubation in normoxia (21% O_2) or in chronic hypoxia (15% O_2) or chronic hyperoxia (30% O_2). Lung morphology (including parabronchial exchange tissues and parabronchial lumina as a percentage of total lung tissue in cross-sectional area, atrial numbers, atrial density) was determined from morphometric examination of thin sections using light microscopy. VEGF expression was determined with ELISA. Body mass was directly correlated with incubation oxygen level, but neither oxygen level affected lung wet mass on either D16 or D18. Hypoxia had little or no effect on most measured pulmonary morphometric indices in D16 embryos. Hypoxia, however, increased by ~65% the proportion in cross-section of the total lung occupied by parabronchi on D18. Hyperoxia caused few significant changes in pulmonary morphometrics. Pulmonary VEGF concentration was decreased by ~30% on day 18 compared to D18 in normoxia. Hypoxia increased pulmonary VEGF concentration by ~35–75% on both D16 and D18 and, paradoxically, VEGF expression was also similarly increased by hyperoxia on only D18. Collectively, these data suggest that pulmonary gross morphological development in the chicken embryo, while moderately plastic, is not profoundly affected by oxygen incubation level, and that role of VEGF in pulmonary development is not yet well understood.

1. Introduction

Birds possess the most structurally complex respiratory system of all air-breathing vertebrates. Several studies have provided details of the gross morphology of the avian pulmonary gas exchange structures (Duncker, 2004; Maina, 2002b, 2006, 2015; Maina et al., 1989, 2010; Maina and Woodward, 2009; West, 2011; Whittow, 2015; Woodward and Maina, 2005, 2008). Briefly, ventilation of the avian lung occurs via a complex system of air sacs, which generate a unidirectional gas flow through the parabronchi of lungs and allows diffusion of gas into the associated air capillaries—the actual site of O_2 and CO_2 exchange (Duncker, 1971; Maina, 2005). Each parabronchus consists of a central lumen, surrounded by a mantle of gas-exchange tissue composed largely of blood and air capillaries. From the lumen of each parabronchus arises invaginations termed atria. These atria lead to smaller funnel-shaped invaginations referred to as infundibula. The air capillaries, which extend from the infundibula, have previously been described as exclusively cylindrical, elongate tubes, but some studies report some or all air capillaries as more globular (rotund) than cylindrical (Maina, 2015; Maina et al., 2010; Maina and Woodward, 2009; Makanya et al., 2011a). Collectively, this complex system of airways ultimately provides for not only the most complex, but also the most efficient, gas exchange organ among air-breathing vertebrates (Maina, 2002a; Makanya et al., 2011a; Scheid, 1979; West, 2009, 2011).

Pulmonary development in bird embryos has been characterized in several studies (Maina, 2003a,b, 2006; Makanya and Djonov, 2009; Makanya et al., 2011b; Mortola, 2009; Mueller et al., 2015; Romanoff, 1960). Pulmonary vasculature is apparent by embryonic day 5 (D5) in chickens, forming by a combination of vasculogenesis and angiogenesis (Mortola, 2009). The airways act as a template for pulmonary blood vessel development, with vessels forming around the airways (Makanya and Djonov, 2009). Sprouting branches

* Corresponding author.
E-mail address: burggren@unt.edu (W.W. Burggren).

http://dx.doi.org/10.1016/j.resp.2015.08.004
1569-9048/

arise from the parabronchial arteries that will eventually surround the parabronchi and then anastomose to form vascular network scaffolding. The pulmonary vasculature undergoes rapid growth through a combination of sprouting and intussusceptive angiogenesis during the last week of incubation (Makanya and Djonov, 2009; Mortola, 2009). A key point in pulmonary development of chicken embryos is achieved around embryonic D16. At this time the interparabronchial septa that separate the parabronchi are developing, and the parabronchi are hexagonal in shape (Maina, 2003a). Formation of the atria in the parabronchi occurs by D15 and infundibula form by D16. The atria extend progressively into the exchange tissue, thereby forming the infundibula, from which air capillaries arise (Maina, 2003b). As development progresses, the epithelium that lines the parabronchial lumen, along with the mesenchymal cells that surround parabronchial tissue, transform into atria, infundibula, and air capillaries. With further pulmonary development, the parabronchial lumen increases in diameter at the expense of the gas exchange tissue mantle (Maina, 2003a). By D18, parabronchus formation is largely complete and the lungs contain well developed atria and infundibula, a wide central lumen, and a thin gas exchange tissue mantle (Maina, 2003a). Air capillaries form by D18 and anastomose profusely in the parabronchi by D20 (Mortola, 2009; Romanoff, 1960).

Normal cardiorespiratory development in bird embryos appears to be somewhat plastic and influenced by environmental conditions, including ambient oxygen, during incubation. In the chicken embryo, chronic hypoxia or hyperoxia causes an often complex suite of changes in the heart, the lungs and the chorioallantoic membrane (Acosta and Hernandez, 2012; Azzam and Mortola, 2007; Chan and Burggren, 2005; Corona and Warburton, 2000; Druyan and Levi, 2012; Wu and Zhang, 2010; Xu and Mortola, 1989; Zhang and Burggren, 2012). In most of these studies organ mass was the primary measured variable, although data specifically on lung mass have only been measured in a few of these studies and very little is known of how the actual morphology, as opposed to the pulmonary mass, changes. Consequently, we still have only rudimentary answers to the question "What is the impact of hypoxia and hyperoxia on the gross morphology of pulmonary development in the bird lung"?

To answer this key question, this study has determined the gross morphological effects on the parabronchial (gas exchange) tissue of the developing lungs of chickens produced by chronic hypoxic and chronic hyperoxic incubation. Based on limited observations of developing vertebrates, changes in ambient oxygen levels have been reported to alter the size and morphology of the gas exchange organ (gills, skin, lungs) (Blank and Burggren, 2014; Burggren and Mwalukoma, 1983; de Meer et al., 1995; Gebb and Jones, 2003; Haworth and Hislop, 2003; Tzaneva et al., 2011). Thus, our first hypothesis was that developmental phenotypic plasticity induced by variations in oxygen level will produce changes to gross morphology of the lung tissues.

The underlying mechanisms for avian cardio-respiratory developmental plasticity in the face of hypoxia are not well understood. Vascular endothelial growth factor (VEGF), a hypoxia-inducible protein, has a broad impact on endothelial cell function, and is critical for development of the lungs in mammals, by inducing angiogenesis and vasculogenesis involved in airway and blood vessel branching (Birk et al., 2008; Bry et al., 2014; Crivellato, 2011; Hines and Sun, 2014; Kumar and Ryan, 2004; Lazarus and Keshet, 2011; Woik and Kroll, 2015). Indeed, at least in developing mammals, the lung has one of the highest levels of VEGF expression among all organs, resulting in a large number of local morphological and physiological effects (Voelkel et al., 2006; Wang et al., 2014). VEGF expression is often found to be induced by hypoxia and inhibited by hyperoxia (Maniscalco et al., 1997; Remesal et al., 2009; Wang et al., 2014). Whether VEGF is similarly implicated in regulation of the development in the avian lung, and how it is affected by tissue oxygenation levels, is less clear. In one of the few studies to look at VEGF expression in the lungs during hypoxic incubation in chicken embryos, VEGF isoforms 122, 146 and 190 were up-regulated by short-term hypoxia at D16, but unchanged at D19 (Been et al., 2010). Consequently, our second hypothesis was that changes in VEGF expression in developing lungs are associated with modifications in morphological development induced by hypoxic or hyperoxic conditions.

2. Materials and methods

2.1. Source and incubation of eggs

Fertilized white Leghorn eggs (*Gallus gallus* variant *domesticus*) were obtained from Texas A&M University and shipped to the University of North Texas, Department of Biological Sciences, where they were placed in Styrofoam egg incubators (1588 Electr. Hova-Bator, G.Q.F. Manuf. Co.). For all groups, eggs were incubated at $37.5 \pm 0.5\,^{\circ}C$ and 55–60% relative humidity (maintained by an open water source in the bottom of the incubator) and were turned automatically every three hours (Tazawa, 1981). Humidity and temperature were constantly monitored within the incubators.

Beginning with onset of incubation (D0), eggs were incubated in one of three treatment groups: normoxia at 21% O_2 (control); chronic hypoxia at 15% O_2; or chronic hyperoxia at 30% O_2. One population was incubated in each condition through D1–16, while the second population was incubated two additional days from D16.

Hypoxic and hyperoxic gases within the incubator were produced by using an on demand servo-null gas regulation system consisting of an oxygen electrode placed within the incubator and a monitoring system and a solenoid system that allowed either N_2 gas (hypoxic conditions) or O_2 gas (hyperoxic conditions) to flow into the incubator as needed to maintain the required oxygenation levels for incubation (15%, 21% or 30% O_2). Gas flow was intermittent (~10–15 s of flow every 1–2 min, with a flow rate of <20 ml/min when solenoids were activated, as dictated by the need to lower PO_2 with N_2, or raise it with O_2. Importantly, this small rate of gas flow was verified as adequate to alter ambient PO_2 without altering incubator temperature.

The University of North Texas' Institutional Animal Care and Use Committee (IACUC) approved all experimental procedures.

2.2. Sampling points during development

Eggs were removed on embryonic days 16 or 18, corresponding to stages 41–43 (Hamburger and Hamilton, 1951), for body mass measurements and collection of lungs for weighing and morphometric measurements. Day 16 was chosen as the first sample point because pulmonary atria and infundibula have formed by D15–D16. D18 was chosen as a second sampling point because by this day of development, a wide central lumen and thin gas exchange tissue mantle is typically present, atria and infundibula are well developed, and most of the parabronchi have formed (Maina, 2003a; Makanya et al., 2013; Makanya and Djonov, 2009). These two sampling points thus encompass the key elements of pulmonary maturation. No measurements were made after D18 because the intent was to avoid any possible changes in pulmonary morphological dimensions associated with the variable, unpredictable levels of actual pulmonary ventilation associated with internal pipping (rupture of the air cell) and lung ventilation beginning on D19 (Xu and Mortola, 1989).

2.3. Tissue collection

Embryos were anesthetized by placing them for 10 min in a closed glass container with gauze pads soaked with isoflurane. Eggs were opened and the deeply anesthetized embryos removed from the shell and separated from the extra-embryonic membranes. The anesthetized embryos were then sacrificed by additional isoflurane exposure or by decapitation. The yolk was removed from the embryonic body, and the yolk-free wet body mass was then measured. The lengths of the beak and the right third toe were measured to the nearest 0.1 mm with calipers to provide an index of development (Chan and Burggren, 2005; Dzialowski et al., 2002; Hamburger and Hamilton, 1951). Embryos were pinned to a dissection tray in a supine position and the coelomic cavity was opened by longitudinal ventromedial incision. The lungs were exposed after careful dissection and reflection of the surrounding structures. Preliminary measurements determined that, due to the fluid-filled and more fragile nature of the embryonic lungs, more consistent results in morphology could be obtained by removing the lungs whole and placing them in fixative, rather than by fixation through intratracheal infusion. Lungs were removed from the body, blotted to remove excess fluids, and wet mass of the lungs was measured. Again, preliminary measurements determined no significant differences between volumes or morphology of gas exchange tissues of right or left lungs. Therefore, routinely the left lungs were chosen for additional morphological analysis.

Lungs were fixed by immersion in 4% paraformaldehyde overnight at 4 °C for preparation of slides for light microscopy examination (see below).

A separate population of birds was used to determine dry mass of the right and left lungs, and the remaining embryo carcass. Tissues were placed in aluminum weighing boats and dried at 60 °C for 24 h, prior to dry weight determination.

2.4. Histology

Embryonic lungs were processed by standard histological methods for light microscopy by dehydration in ethanol followed by embedding *in toto* in paraffin wax (Maina, 2002b, 2003a,b; Maina et al., 1989). Some shrinkage inevitably occurs in pulmonary tissues due to histological processing. It was assumed that the different morphological components of the avian lung shrink equivalently, maintaining the same relative proportions when examined histologically.

Following histological preparation, each lung was serially sectioned at 5 μm intervals transversely to the long axis of the lung. Sections were then stained using conventional hematoxylin and eosin stains. Sections were determined to be technically adequate and fixation satisfactory when the lumina of the parabronchi were patent and the exchange tissue was intact (Maina, 2002b; Maina et al., 1989).

2.5. Morphometric measurements

2.5.1. Thin section selection

Each lung yielded 8–12 thin sections when serially sectioned equidistantly through the lung tissue. For morphometric analysis, one thin section was chosen consistently from the same location of each lung, midway through the lung (middle third along the long axis) typically at a distance of 1.10–2.40 mm from the lung tip, depending on the lung's total length. The 4th, 5th, or 6th thin section was typically chosen, corresponding to the lung midpoint. The midpoint was chosen because the thin sections taken from this portion of the lung were the largest and most consistent in structure, spanning the entire cross-section of the lung without breaks in the tissue. The midpoint thin sections were, therefore, the most histologically appropriate with intact parabronchial tissue, as well as the most homogenous in nature, when using entire cross-sections for analysis and comparison (see below).

Each thin section was photographed using an Olympus DP70 digital camera system mounted on to a Nikon Eclipse E200 light microscope. All sections were photographed at a total magnification of 40×, and subsequent analyses were made using ImageJ software (National Institutes of Health).

2.5.2. Lung surface area relationships

Imaging software was used to trace the outer edges of the tissue thin section on the glass slide and then calculate the tissue surface area within the tracing. This value for lung tissue surface area as presented on the slide was determined for each thin section, and then served as the reference used to determine the fractional percentage of this total area that was actually occupied by specific lung tissue types.

The components of lung tissue thin section that were assessed for relative surface area were the lumina, the parabronchi alone, the parabronchi plus lumina, and the non-parabronchial tissue. The percentage of each pulmonary tissue component, determined from the thin section surface areas, was calculated using the following formula:

$$\text{Component\%} = \left(\frac{SA_{comp}}{SA_{lung}}\right) \times 100$$

where

- SA_{lung} is the entire surface area of the lung thin section determined by tracing around the entire outside edge of the lung tissue on the slide (see above), and
- SA_{comp} is the surface area in thin section of the specific component (*e.g.*, lumina) within the entire lung thin section, determined by tracing around all occurrences of that component within the total tissue used to determine SA_{lung}.

To determine the percentage that the lumina of the parabronchi occupied within each lung thin section in histological cross-section, the outside edge of each lumen was traced, as illustrated in Fig. 1. The sum of each individual lumen surface area was then used to determine the percentage of lung tissue consisting of lumina.

To determine the percentage of total lung tissue of the parabronchi plus lumina within each lung section, the outside edges of all parabronchial tissue were traced (Fig. 1). The parabronchi included the secondary bronchi because of their resemblances in having a mantle of exchange tissue, which make them functionally similar and difficult to distinguish on histological sections (Maina et al., 1989). After tracing all parabronchial tissue, the sum of all individual parabronchial surface area measurements was then used to determine the percentage of total lung tissue in cross-sectional area that comprised parabronchial tissue. Additional calculations from these primary data included thin section surface area of all parabronchi including lumina, parabronchi without lumina, and non-parabronchial tissue.

2.5.3. Blood vessel density

The density of all visible blood vessels (arteries, arterioles, venules and veins), was counted for each thin section, and expressed as number of vessels per mm^2 of tissue thin section (Fig. 1). Because this study was limited to light microscopy, individual capillaries could not be clearly visualized, and so were not counted.

2.5.4. Atria density and lumina circumference

For each thin section, the measurements of luminal circumference and atrial density were taken within a 1 mm^2 field of view

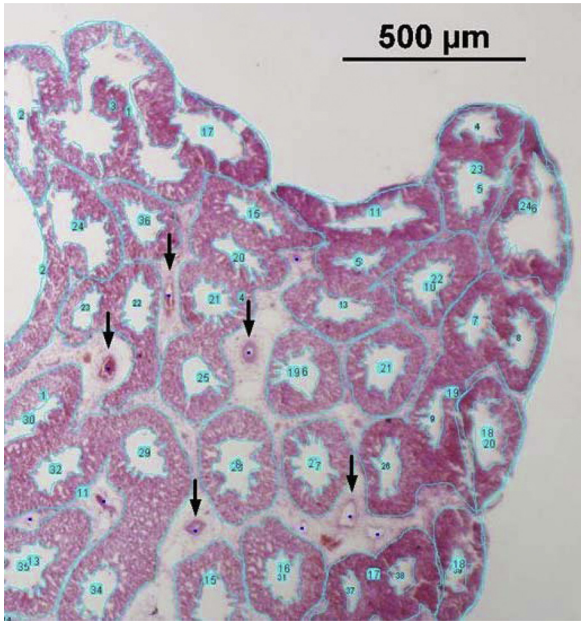

Fig. 1. Methodology for determining two dimensional surface area of the entire tissue of each thin section. The entire surface area for each tissue thin section was determined by tracing around the outer edges of the tissue on the slide (light blue line). This served as the reference for calculating the percentage of slide area occupied by lumina, parabronchi, parabronchi plus lumina, and non-parabronchial tissue of total lung tissue (only a portion of a complete section is shown in this figure, for clarity). The outside edge of each lumen of the parabronchus was then traced to determine luminal surface area, with each lumen being assigned a unique number by the image analysis software. Then, the outside edges of all parabronchi were traced to determine parabronchial tissue surface area. (In this image, the process of parabronchial tracing created a second unique set of numbers for each parabronchus, resulting in occasional overlapping numbers reflecting the two stage analysis process.) Representative major blood vessels are indicated by arrows. See text for additional details (For interpretation of the references to color in this figure legend, the reader is referred to the web version of this article.).

located in the second third of the lateral region of the lung. This measurement was taken from within a 1 mm^2 field of view to achieve a greater precision in tracing all atria and infundibula than could be achieved with more generalized luminal tracings from entire sections. The circumference of each lumen was determined by tracing the edges of each lumen, including all atria and infundibula (Fig. 2). All lumina circumferences were then summed to determine the total luminal circumference, expressed as mm of circumference per mm^2 of thin section area.

Atria were defined by the presence of distinct invaginations deviating from the smooth, spherical shape of the lumen. Infundibula that invaginated from the atria were not counted separately from the originating atria. The number of atria of all lumina (Fig. 2 inset) was summed to determine total atria, expressed as number of atria per mm^2 of tissue thin section.

2.6. Pulmonary VEGF concentration

After measurement of wet mass, the right lung of each embryo was used to measure VEGF concentration. Lungs were placed in vials containing saline, flash frozen in liquid nitrogen, and stored at −80 °C for later analysis. Frozen lungs were then homogenized in buffer (490 µL protein extraction reagent, 5 µL protease inhibitor cocktail, 5 µL EDTA) and centrifuged at 10,000 RPM for 5 min. The VEGF concentrations of the homogenates were determined with a double-antibody sandwich enzyme-linked immunosorbent assay (ELISA) kit (NovaTeinBio, Woburn, Massachusetts, USA) specific to the chicken VEGF protein. In brief, following centrifugation, 10 µL of supernatant and 40 µL of sample diluent were added in duplicate to a 96 well plate coated with a monoclonal antibody for chicken VEGF. The well plate was then incubated at 37 °C for 30 min. Following four washes using a proprietary solution provided by NovaTeinBio to remove unbound substances, 100 µL of HRP conjugate reagent (VEGF antibody and horseradish peroxidase) was added to each well and incubated at 37 °C for 30 min. Following four additional washes to remove unbound antibody-HRP (horse radish peroxidase), the kit's color reagents (chromogenic substrate A and B—50 µL each) were added to each well and incubated at 37 °C for 15 min. Then 50 µL of stop solution was added to each well. The optical density was measured at 450 nm in a microplate reader within 15 min of the addition of stop solution. For standardization, calibration standards for chicken VEGF, supplied by the manufacturer, were added in duplicate to additional wells at the same time as the supernatant and sample diluents.

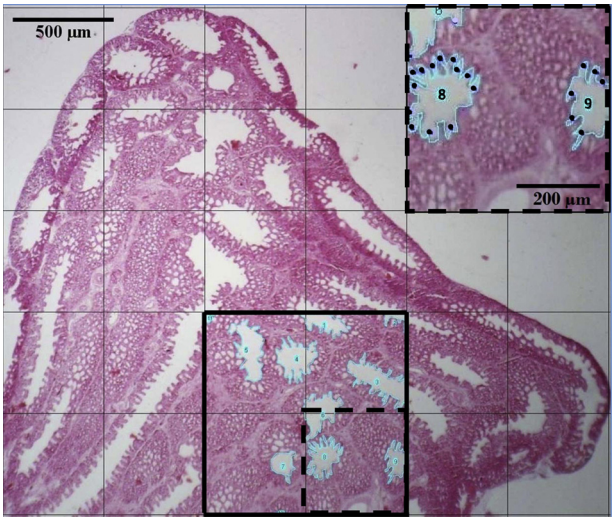

Fig. 2. Characteristics of the lumina. The light weight grid lines enclose areas 0.5 mm × 0.5 mm on edge. For each histological section, measurements were taken from a 1 mm^2 field (outlined by medium weight line in the bottom central region of figure) located laterally in the second third of the lung. The inset in the upper right is blown up from the area outlined by the dashed lines within the 1 mm^2 field. Lumina circumference was determined by tracing the edges of each lumen, including all atria and infundibula, and summed to determine luminal circumference (mm per mm^2 of tissue thin section). In this particular slide, the 1 mm^2 field of view contained all or part of nine lumina (numbered). Luminal atria (indicated by dots) were counted to determine total atria per mm^2 of tissue thin section.

All calculated VEGF concentrations were determined using a standard curve calculated from the supplied calibration standards by plotting the mean absorbance for each standard against the concentration, determining the best fit curve to obtain the linear regression equation, and then calculating each actual sample concentration using its optical density and linear regression equation. Then each calculated concentration per sample was divided by the mass of the lung tissue actually in that sample.

2.7. Statistical analysis

All data were tested for normality of distributions (Shapiro–Wilk test) prior to other statistical tests. Data were analyzed using two-way ANOVAs with embryo age and oxygen level as the two factors. A significance level of 0.05 was used followed by Tukey's post-hoc tests. Statistics were performed using SigmaPlot 12. All data are presented as means ± standard error.

3. Results

Mean values, *n* values and statistics of control values (normoxia) measured variables and the differential changes induced by chronic

Table 1
Differential responses of body mass, pulmonary mass and length of beak and toe to incubation in normoxia, chronic hypoxia and hyperoxia in D16 and D18 embryos. Data are presented as mean ± SE. *N* values are in parentheses. Bold indicates values for hypoxia or hyperoxia that are significantly different ($p < 0.05$ or smaller) from normoxia (control) values at the same day of development. See text for additional details of statistical testing.

Embryonic age (DPF)	D16			D18			Statistics for two-way ANOVA on development and oxygen level	
Oxygen level (%)	15	21 (control)	30	15	21 (control)	30	*p* value for O_2 effect	*p* value for day effect
Embryo wet mass (g)	**13.7 ± 0.6** (7)	14.5 ± 0.9 (8)	**16.7 ± 0.2** (7)	**19.1 ± 0.8** (6)	21.3 ± 1.5 (10)	21.2 ± 0.9 (13)	<0.001	<0.001
Embryo dry mass (g)	**1.9 ± 0.2** (**7**)	2.4 ± 0.3 (8)	**2.5 ± 0.1** (7)	**3.2 ± 0.1** (6)	4.2 ± 0.5 (10)	4.1 ± 0.2 (13)	<0.001	<0.001
Lung wet mass (mg)	114.3 ± 12.1 (7)	136.3 ± 9.8 (8)	155.7 ± 10.7 (7)	180.0 ± 17.6 (6)	196.0 ± 16.4 (10)	205.2 ± 14.8 (13)	NS	<0.001
Lung dry mass (mg)	**14.0 ± 1.6** (10)	17.5 ± 1.5 (10)	**19.5 ± 1.2** (8)	24.5 ± 3.0 (9)	27.9 ± 2.6 (10)	29.4 ± 2.0 (10)	NS	<0.001
Wet lung mass-to-wet embryo mass ratio (×100)	0.94± 0.09 07char_dotchar_(7)	0.87 ± 0. 07 (8)	0.99 ± 0.07 (7)	1.01 ± 0.12 (6)	0.83 ± 0.06 (10)	0.67 ± 0.13 (13)	NS	<0.05
Dry lung mass-to-dry embryo mass ratio (×100)	0.72 ± 0.04 (7)	0.77 ± 0.06 (8)	0.79 ± 0.06 (7)	0.78 ± 0.10 (6)	0.70 ± 0.06 (10)	0.72 ± 0.04 (13)	NS	NS
Beak length (mm)	**3.4 ± 0.2** (10)	4.0 ± 0.1 (10)	3.7 ± 0.1 (8)	4.5 ± 0.1 (7)	4.6 ± 0.1 (10)	4.7 ± 0.1 (10)	NS	<0.001
Toe length (mm)	**13.1 ± 0.3** (10)	14.5 ± 0.2 (10)	14.7 ± 0.2 (8)	**16.4 ± 0.1** (7)	18.3 ± 0.4 (10)	18.2 ± 0.3 (10)	<0.001	<0.001

Table 2
Differential responses of pulmonary morphometrics and VEGF expression of parabronchial lungs to incubation in chronic hypoxia and hyperoxia in D16 and D18 embryos. Data are presented as mean ± SE. *N* values are in parentheses. Bold indicates values in hypoxia or hyperoxia that are significantly different ($p < 0.05$) from normoxia (control) values at the same day of development. See text for additional details of statistical testing.

Embryonic age (DPF)	D16			D18			Statistics for two-way ANOVA on development and oxygen level	
Oxygen level (%)	15	21	30	15	21	30	*p* value for O_2 effect	*p* value for day effect
Parabronchial tissue (% of total pulmonary tissue)	60.8 ± 1.9 (6)	63.7 ± 3.2 (6)	66.3 ± 1.1 (7)	**68.2 ± 1.8** (6)	62.8 ± 2.3 (6)	66.7 ± 2.0 (6)	<0.02	<0.005
Lumina (% of total pulmonary tissue)	13.4 ± 1.6 (6)	14.2 ± 1.8 (6)	14.1 ± 1.3 (6)	13.9 ± 1.4 (6)	16.5 ± 2.0 (6)	18.6 ± 1.9 (6)	NS	NS
Parabronchi plus lumina (% of total pulmonary tissue)	74.2 ± 2.5 (6)	78 ± 1.8 (6)	**80.4 ± 0.7** (6)	82.2 ± 2.0 (6)	79.4 ± 1.6 (6)	**85.2 ± 1.0** (7)	<0.02	<0.005
Non-parabronchial tissue (% of total pulmonary tissue)	25.8 ± 2.5 (6)	22.0 ± 1.8 (6)	**19.6 ± 0.7** (6)	17.9 ± 2.0 (6)	20.7 ± 1.6 (6)	**14.8 ± 1.0** (7)	<0.002	<0.005
Luminal circumference (mm per mm^2)	11.7 ± 2.3 (6)	11.5 ± 2.1 (6)	13.6 ± 2.3 (6)	11.9 ± 1.4 (6)	10.6 ± 1.4 (6)	10.8 ± 1.6 (6)	NS	NS
Number of atria (per mm^2)	73.1 ± 13.9 (6)	67.8 ± 10.4 (10)	88.7 ± 17.3 (13)	132.8 ± 7.1 (6)	136.7 ± 18.2 (8)	131.7 ± 21.6 (7)	NS	<0.001
Atrial density (per mm^2)	6.8 ± 1.0 (6)	6.1 ± 0.6 (6)	6.5 ± 0.9 (6)	11.6 ± 0.9 (6)	13.1 ± 1.2 (6)	12.3 ± 1.1 (6)	NS	<0.001
Blood vessels (per mm^2)	2.8 ± 0.4 (6)	2.4 ± 0.4 (6)	2.7 ± 0.3 (6)	2.2 ± 0.2 (6)	3.5 ± 0.5 (6)	2.8 ± 0.5 (7)	NS	NS
VEGF (pg/mL)	**736 ± 91.4** (7)	538.8 ± 32.4 (6)	480.0 ± 28.0 (6)	**631.4 ± 8.0** (7)	380.5 ± 36.6 (7)	**672.5 ± 75.6** (7)	<0.002	NS

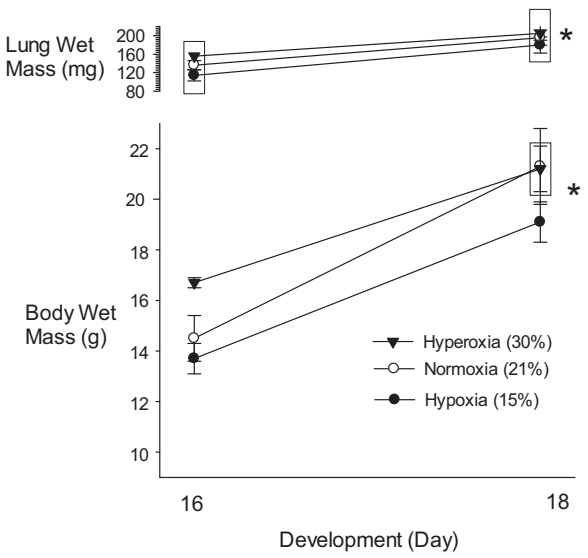

Fig. 3. Wet mass of lung and whole yolk-free embryo as a function of incubation oxygen level (chronic hypoxia, normoxia, or hyperoxia) and development from embryonic day 16 to 18 in chicken embryos. Sample sizes are provided in Table 1. Data are presented as mean ± SE. An asterisk indicates a significant difference between developmental days as determined by a two way ANOVA (see text for additional details). Boxes enclose means at any given day of development that are not significantly different from each other.

hypoxic or hyperoxic incubation are provided in Tables 1 and 2. Table 3 provides a summary of the direction of change for each variable, at each day, for each incubation condition.

3.1. Embryo mass

Embryo wet mass increased significantly with development from D16 to D18 for all three treatment groups (Table 1, Fig. 3). Chronic hypoxic incubation reduced body mass compared to normoxic embryos at both D16 and D18. In contrast, on D16 (but not D18) the wet mass of hyperoxic embryos was significantly greater compared to normoxic controls. Additionally, embryo dry mass showed exactly the same pattern of changes with hypoxic and hyperoxic incubation as wet mass, suggesting that there was no significant edema or dehydration caused by any of the incubation protocols.

3.2. Beak and toe length

Beak length and toe length both increased significantly ($p < 0.001$) with development from D16 to D18 for all oxygen levels (Table 1). Beak and toe length were reduced in the hypoxic group compared to the normoxic group on D16. There were no differences in beak length between normoxic and hyperoxic incubation groups on D16, nor between any oxygen incubation group on D18 (Table 1). On D18, toe length was significantly lower than control, with hyperoxia having no effect (Table 1). Collectively, these data indicate that hypoxia induced a small developmental delay up to D16, with some recovery in developmental stage evident two days later at D18.

3.3. Pulmonary tissue masses

Lung wet mass increased with development from D16 to D18 at all three oxygen incubation levels, but there were no differences in lung wet mass between oxygen levels on either sampling day (Table 1, Fig. 3). The ratio of lung wet mass to embryo wet mass in control embryos was 0.0099 ± 0.0016 on D16 and 0.0083 ± 0.0006

Table 3
Summary of differential responses of pulmonary morphometrics and VEGF expression of parabronchial lungs to incubation in chronic hypoxia and hyperoxia in D16 and D18 embryos. All changes are expressed relative to normoxic controls. See Tables 1 and 2 for mean values, *n* values and statistics.

Embryonic age	Condition	Measured variables (change relative to normoxic controls at designated day of development)																
		Embryo wet mass (g)	Embryo dry mass (g)	Lung wet mass (mg)	Lung dry mass (mg)	Wet lung mass-to-wet embryo mass ratio (×100)	Dry lung mass-to-dry embryo mass ratio (×100)	Beak length (mm)	Toe length (mm)	Parabronchial tissue (% of total pulmonary tissue)	Parabronchial lamina (% of total pulmonary tissue)	Parabronchial plus lumina (% of total pulmonary tissue)	Non-parabronchial tissue (% of total pulmonary tissue)	Luminal fractional cumference (mm per mm^2)	Number of atria (per mm^2)	Atrial density (per mm^2)	Blood vessels (per mm^2)	VEGF (pg/mL)
Day 16	Hypo	→	→	–	→	–	–	→	→	–	–	–	–	–	–	–	–	↑
	Hyper	↑	↑	–	↑	–	–	–	–	–	–	↑	↓	–	–	–	–	–
Day 18	Hypo	→	→	–	–	–	–	–	→	↑	–	–	–	–	–	–	–	↑
	Hyper	–	–	–	–	–	–	–		–	–	↑	↓	–	–	–	–	↑

on D18 (Table 1), and was not affected by oxygen incubation level on either day of sampling.

Lung dry mass increased significantly ($p < 0.01$) with development for all oxygen levels (Table 1), and oxygen incubation level had no effect on lung dry mass at either D16 or D18. The ratio of lung dry mass to embryo dry mass, as for this ratio for wet masses, was 0.0169 ± 0.0273 on D16 and on 0.0272 ± 0.0012 on D18, and was not affected by oxygen incubation level.

The ratio of dry lung mass to wet lung mass increased from day 16 (0.129 ± 0.010) to day 18 (0.143 ± 0.004), indicating a slightly lower water content with the additional maturation of the lungs over these two days. There was, however, no significant effect of oxygen level at either day of development.

3.4. Pulmonary morphometrics

Changes in pulmonary morphometrics as a function of development and incubation oxygen levels are presented in Table 2. There were no differences in the percentage of parabronchi as a percentage of total lung tissue in thin section, between D16 and D18 for control (normoxic) embryos (Table 2). At D16, neither hypoxia nor hyperoxia had any effect on parabronchial tissue percentage. However, on D18 the parabronchial proportion (expressed as a percentage) increased from the normoxic value of ~63% of total lung tissue up to ~68% in the hypoxic population (Table 2).

The percentage of total pulmonary tissue occupied by lumina was not significantly affected by either day of development or level of oxygen incubation (Table 2).

The percentage of total pulmonary tissue occupied by the parabronchi plus lumina increased significantly from D16 to D18 in all populations. Hyperoxia, but not hypoxia, increased this variable at both D16 and D18 (Table 2).

The percentage of non-parabronchial tissue in the lungs of normoxic embryos was ~21–22% on both days of development. However, this variable was decreased by hyperoxia on both D16–D18 (Table 2).

Total luminal circumference (mm of circumference per mm^2 of tissue thin section) was not affected by day of development or incubation oxygen level (Table 2).

The number of atria per mm^2 lung thin section and the calculated atrial density nearly doubled from D16 to D18 in all three incubation populations (Table 2). However, incubation oxygen level itself had no effect on atrial numbers or density at either day of development.

Blood vessel density (number of blood vessels per mm^2 tissue thin section) were not affected by developmental days or oxygen levels (Table 2).

3.5. Pulmonary VEGF concentration

Pulmonary VEGF concentration in the normoxic population decreased by ~30% from day 16 to 18 (Table 2, Fig. 4). On D16, VEGF concentration was approximately 35–40% higher in the hypoxic group compared to the control and hyperoxic groups, which were not different from each other (Table 2, Fig. 4). On Day 18, pulmonary VEGF concentration in the hypoxic and hyperoxic group was elevated 66% and 76% above the control group, respectively.

4. Discussion

This study has investigated the morphological effects of variations in O_2 level on chicken embryos and their morphology, especially of the lungs. The effects did not reflect simple dose–response relationships, as will now be discussed.

4.1. Wet and dry embryo mass

The increase in both embryo and lung wet mass for all O_2 level groups from D16 to D18 was as anticipated, reflecting continuing embryonic growth during late development as a prelude to internal pipping and pulmonary ventilation. The present study has shown that hypoxic incubation from D1–D18 reduces embryo wet mass, confirming previous studies (Altimiras and Phu, 2000; Burton and Palmer, 1992; Chan and Burggren, 2005; Copeland and Dzialowski, 2009; Dzialowski et al., 2002; Molenaar et al., 2011; Stock and Metcalfe, 1987; Xu and Mortola, 1989; Zhang and Burggren, 2012). Collectively, these data suggest that O_2 availability at even relative modest hypoxia (15% O_2) significantly limits embryonic growth, and that no particular critical window during development for the hypoxic retardation of growth. Embryo mass also increases in chronic hyperoxia, suggesting that there is an oxygen limitation to growth within the egg during normoxia (Copeland and Dzialowski, 2009). Hyperoxia also stimulated growth in the present study on D16, but not on D18 of development (Table 1), indicating a likely plateauing of growth – even in the presence of an abundance of oxygen – as internal pipping approaches.

Dry embryo masses reflected the same trends as wet embryo mass, with no significant differences in dry embryo-to-wet embryo mass ratios, indicating no overall tissue edema caused by variable O_2 levels.

4.2. Beak and toe length

Beak and toe length is a commonly used indicator of developmental stage (Hamburger and Hamilton, 1951). As with the overall increase in body mass with development, the significant increase in both beak and toe length for all O_2 level groups from D16 to D18 was anticipated to occur as a result of normal developmental growth over time. Hypoxia reduced beak and toe length (Table 1), indicating a possible hypoxia-induced developmental delay. These findings align with other studies describing smaller but also less mature embryos under hypoxic incubation (Azzam et al., 2007; Copeland and Dzialowski, 2009; Dzialowski et al., 2002; Xu and Mortola, 1989). Using normal tables of chicken development (Hamburger and Hamilton, 1951), the differences in beak and toe length for hypoxic embryos in this study on both D16 and D18 indicate a developmental delay of ~24 h. This is consistent with the observation that embryos incubated in hypoxic conditions tended to internally pip one day later than those incubated in normoxic and hyperoxic conditions (Copeland and Dzialowski, 2009).

4.3. Pulmonary developmental plasticity

4.3.1. Pulmonary mass

One of the key questions of this study was whether hypoxia might stimulate or inhibit pulmonary growth, either of which would be evidence of environmentally-induced developmental phenotypic plasticity of the embryonic respiratory system. The results of the present study support previous studies showing that embryonic lung mass is only modestly affected, if affected at all, by hypoxic incubation (Chan and Burggren, 2005; Xu and Mortola, 1989). Yet, in the present and previous studies there is clear evidence for oxygen level-induced developmental plasticity of the toes, beak and other organs. Thus, the developmental trajectory for the embryonic lungs in particular appears to be more fixed than for other organs, which we speculate may result from the utter importance of having lungs with a respiratory surface area sufficient to carry out respiration in the perinatal period and into adulthood. Noteworthy, however, is that in a previous study considering lung mass during development in chicken embryos (Xu and Mortola, 1989), hypoxic incubation actually did increase the lung to body

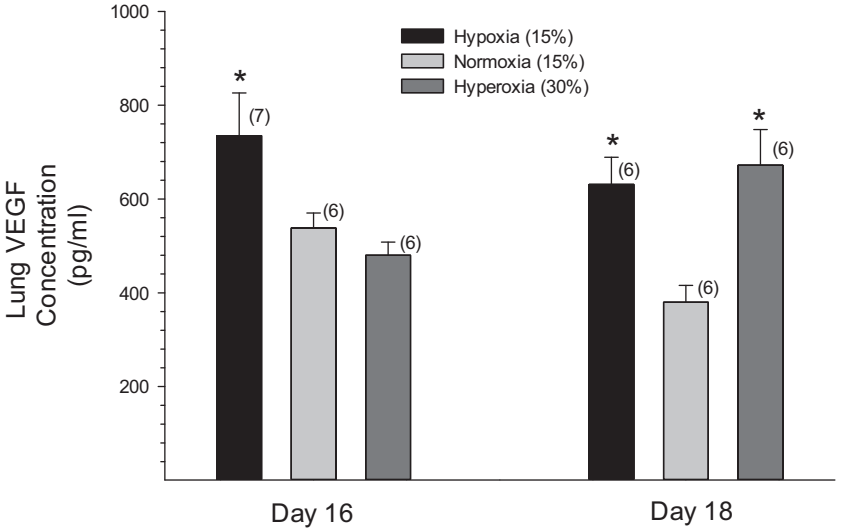

Fig. 4. Lung VEGF concentration on embryonic days 16 and 18 in the chicken embryo exposed to chronic hypoxia, normoxia, or hyperoxia. Data are presented as mean ± SE. *N* values are in parentheses. An * indicates significant difference from the normoxic (control) value.

mass ratio, but the more extreme hypoxic level of that study (10% O_2) also caused a larger decrease in embryo mass. There may, in fact, be a hypoxic threshold for pulmonary developmental plasticity, and we would argue for the construction of "dose-response" curves in future studies that document the potentially variable effects of variable oxygen levels.

4.3.2. Lung morphology

The structure of the lung of the adult bird has been characterized in detail (Maina, 2003a,b, 2006; Makanya and Djonov, 2009; Makanya et al., 2011b; Mortola, 2009; Mueller et al., 2015; Romanoff, 1960; Stock and Metcalfe, 1987). However, poorly understood is the development of these internal pulmonary tissues and related structures and how they are affected by O_2 incubation level. During normal development there is an increase in parabronchial tissue and a decrease of non-parabronchial tissue as a percentage of total lung tissue, reflecting the maturation of the lungs toward the necessity of pulmonary respiration at internal pipping (Maina, 2003a; Whittow, 2015). We hypothesized that incubation in chronic hypoxia or hyperoxia would primarily alter the parabronchial tissue as the actual site for pulmonary gas exchange. In fact, chronic hypoxic incubation caused no change in the percentage of parabronchial tissue (with or without lumina included) on D16. By Day 18, however, hypoxic incubation had significantly increased the percentage of parabronchial tissue. Given that internal pipping could occur as early as D19, this increase in parabronchial tissue could signal an increase in the gas exchange of the lung as pulmonary respiration begins.

Parabronchial lumina increase in diameter as the chicken embryo's lungs develops (Maina, 2003a), but in the current study, factors related to parabronchial luminal diameter were unaffected with late development from D16 to D18. Incubation O_2 level did not affect the percentage of lung tissue occupied by lumina. An increase in the number of luminal atria is also expected to occur as development progresses (Maina, 2003b), and the current study revealed that atrial numbers and atrial density increased with development (Table 2), approximately doubling just between D16 and D18. These data suggest that a considerable amount of the normal maturational increase in respiratory surface area occurs in the final few days before the onset of pulmonary ventilation. Interestingly, however, neither chronic hypoxia nor hyperoxia altered these variables on either D16 or D18, suggesting a fixed developmental trajectory for these pulmonary tissues irrespective of oxygen availability.

Adaptive changes in pulmonary surface area ideally should match increased pulmonary vascularization to maintain optimal perfusion–diffusion ratios and hence maximize gas exchange effectiveness. In our study, blood vessel density was unaffected by developmental stage or O_2 level, suggesting that vascularization (at least, of the major blood vessels that we observed) kept pace with atrial proliferation.

4.4. VEGF concentration

Hypoxia-inducible factors (HIF-1 and HIF-2) are regulatory proteins controlling expression of most genes involved in hypoxia adaptation. HIF is heavily involved in the expression of VEGF (Berchner-Pfannschmidt et al., 2008; Bigham and Lee, 2014; Garcia et al., 2015; Gorr et al., 2010; Prabhakar and Semenza, 2012; Taylor and McElwain, 2010; van Patot and Gassmann, 2011; Xiao, 2015). Hypoxia increases concentrations of HIF-1, which in turn stimulates VEGF transcription (Garcia et al., 2015; Padmanabha et al., 2015; Woik and Kroll, 2015). A primary action of VEGF is to stimulate blood vessel formation and thus potentially increase the perfusion and thus oxygenation in a wide range of tissues (Burggren, 2013; Clerici and Planes, 2009; Voelkel et al., 2006). VEGF also has pivotally important roles in the induction of the necessary angiogenesis and vasculogenesis involved in not only blood vessel branching, but also airway branching in the mammalian lung (Birk et al., 2008; Bry et al., 2014; Crivellato, 2011; Hines and Sun, 2014; Hislop, 2005; Kumar and Ryan, 2004; Lazarus and Keshet, 2011; Tuder et al., 2007; Woik and Kroll, 2015).

Because of the above-mentioned actions of VEGF and its relation to tissue hypoxia, we hypothesized that VEGF concentration would increase in lung tissues exposed to chronic hypoxia, and decrease in lung tissues exposed to chronic hyperoxia. Indeed, on both D16 and D18 VEGF was considerably elevated in the hypoxic group compared to the control and hyperoxic group (Table 2, Fig. 4). The major pulmonary blood vessels showed no evidence of an O_2 level incubation effect in this study, but the smallest gas exchange vessels may have been stimulated by hypoxia during this developmental period, which could produce a greater perfusion of the pulmonary gas exchange surfaces.

It was additionally hypothesized that VEGF concentration would decrease under hyperoxia as a consequence of decreased HIF-1 expression. Certainly, in neonatal mammals hyperoxia suppresses VEGF expression (Fujinaga et al., 2009; Keenaghan et al., 2013).

However, hyperoxia has also been found to enhance VEGF release from cell-associated stores, as a potential adaptive response to hyperoxia-induced cell injury (Shenberger et al., 2007), and VEGF potentially has other beneficial developmental effects in hyperoxia (Bhandari et al., 2008). In the present study, VEGF expression in hyperoxia did not differ from normoxia on D16, yet, was actually ~75% *higher* in hyperoxia than in normoxia on day 18. The reasons for this are unclear. Chicken eggs exposed to hyperoxia from days 7 to 14 of development exhibit a decreased rate of growth by extraembryonic blood vessels of the chorioallantoic membrane (the main gas exchange organ of the avian embryo) as well as destruction of the capillary plexus, in an O_2 dose-related manner (Strick et al., 1991). Perhaps hyperoxic exposure during incubation actually decreases the gas-exchange capabilities of the CAM, ironically resulting in an internally hypoxic environment for the embryo and its pulmonary tissues during hyperoxic incubation. This could, in turn, result in a stimulation of pulmonary VEGF expression, as seen in this study on D18.

Given the demonstration of major changes in VEGF concentration as a function of both late embryonic development and developmental stage, a study of the correlation of VEGF with pulmonary gross anatomy is highly warranted.

4.5. Future directions

This study has generated several key questions. Does chronic hypoxic exposure in development affect the gas exchange tissue in the avian lungs in ways that actually alter pulmonary gas exchange upon internal and then external pipping? Does the gas exchange effectiveness of the CAM, which also changes with hypoxic exposure (Chan and Burggren, 2005; Strick et al., 1991), influence developmental plasticity of the parabronchial lungs? Finally, what are the critical windows, if any, for modification of pulmonary development? Developmental critical windows will surely exist for pulmonary morphology, as they do for other structures (Burggren and Reyna, 2011; Burggren, 2015; Symonds et al., 2007), but the delineation of the limits or "edges" of these windows is likely highly dependent on hypoxia level (dose) used in a particular study (Burggren and Mueller, 2015). Unfortunately, however, there is currently no "industry standard" level (dose) of hypoxia used in incubation protocols for chicken embryos—different studies variously use O_2 incubation levels of 10%, 12%, 14% and 15%. Future studies on the effect of environmental stressors on embryonic development will be even more useful if they employ multiple stressor doses within experimental design.

Acknowledgement

This study was prepared with the support of grant IOS-1025823 to WB from the U.S. National Science Foundation.

References

Acosta, E., Hernandez, A., 2012. Vascular density, hypoxia inducible factor, vascular endothelial growth factor, and its receptor expression in the chorioallantois of relatively normoxic and hypoxic chicken embryos, at 6 and 7 days of incubation, and corresponding weight values. Poult. Sci. 91, 2637–2644.

Altimiras, J., Phu, L., 2000. Lack of physiological plasticity in the early chicken embryo exposed to acute hypoxia. J. Exp. Zool. 286, 450–456.

Azzam, M.A., Mortola, J.P., 2007. Organ growth in chicken embryos during hypoxia: implications on organ sparing and catch-up growth. Respir. Physiol. Neurobiol. 159, 155–162.

Azzam, M.A., Szdzuy, K., Mortola, J.P., 2007. Hypoxic incubation blunts the development of thermogenesis in chicken embryos and hatchlings. Am. J. Physiol. Regul. Integr. Comp. Physiol. 292, R2373–R2379.

Been, J.V., Zoer, B., Kloosterboer, N., Kessels, C.G., Zimmermann, L.J., van Iwaarden, J.F., Villamor, E., 2010. Pulmonary vascular endothelial growth factor expression and disaturated phospholipid content in a chicken model of hypoxia-induced fetal growth restriction. Neonatology 97, 183–189.

Berchner-Pfannschmidt, U., Frede, S., Wotzlaw, C., Fandrey, J., 2008. Imaging of the hypoxia-inducible factor pathway: insights into oxygen sensing. Eur. Respir. J. 32, 210–217.

Bhandari, V., Choo-Wing, R., Lee, C.G., Yusuf, K., Nedrelow, J.H., Ambalavanan, N., Malkus, H., Homer, R.J., Elias, J.A., 2008. Developmental regulation of NO-mediated VEGF-induced effects in the lung. Am. J. Cell Respir. Mol. Biol. 39, 420–430.

Bigham, A.W., Lee, F.S., 2014. Human high-altitude adaptation: forward genetics meets the HIF pathway. Genes Dev. 28, 2189–2204.

Birk, D.M., Barbato, J., Mureebe, L., Chaer, R.A., 2008. Current insights on the biology and clinical aspects of VEGF regulation. Vasc. Endovasc. Surg. 42, 517–530.

Blank, T., Burggren, W., 2014. Hypoxia-induced developmental plasticity of the gills and air-breathing organ of *Trichopodus trichopterus*. J. Fish Biol. 84, 808–826.

Bry, M., Kivela, R., Leppanen, V.M., Alitalo, K., 2014. Vascular endothelial growth factor-B in physiology and disease. Physiol. Rev. 94, 779–794.

Burggren, W.W., 2013. Cardiovascular development and angiogenesis in the early vertebrate embryo. Cardiovasc. Eng. Technol. 4, 234–245.

Burggren, W.W.a., 2015. Developmental critical windows and sensitive periods as 3-D constructs in time and space (invited perspective). Physiol. Biochem. Zool. 88, 91–102.

Burggren, W., Mwalukoma, A., 1983. Respiration during chronic hypoxia and hyperoxia in larval and adult bullfrogs (*Rana catesbeiana*). I. Morphological responses of lungs, skin and gills. J. Exp. Biol. 105, 191–203.

Burggren, W.W., Mueller, C.A., 2015. Developmental critical windows and sensitive periods as 3-D constructs in time and space (invited perspective). Physiol. Biochem. Zool. 88 (2), 91–102.

Burggren, W.W., Reyna, K.S., 2011. Developmental trajectories, critical windows and phenotypic alteration during cardio-respiratory development. Respir. Physiol. Neurobiol. 178, 13–21.

Burton, G.J., Palmer, M.E., 1992. Development of the chick chorioallantoic capillary plexus under normoxic and normobaric hypoxic and hyperoxic conditions: a morphometric study. J. Exp. Zool. 262, 291–298.

Chan, T., Burggren, W., 2005. Hypoxic incubation creates differential morphological effects during specific developmental critical windows in the embryo of the chicken (*Gallus gallus*). Respir. Physiol. Neurobiol. 145, 251–263.

Clerici, C., Planes, C., 2009. Gene regulation in the adaptive process to hypoxia in lung epithelial cells. Am. J. Physiol. Lung Cell. Mol. Physiol. 296, L267–L274.

Copeland, J., Dzialowski, E.M., 2009. Effects of hypoxic and hyperoxic incubation on the reactivity of the chicken embryo (*Gallus gallus*) ductus arteriosi in response to catecholamines and oxygen. Exp. Physiol. 94, 152–161.

Corona, T.B., Warburton, S.J., 2000. Regional hypoxia elicits regional changes in chorioallantoic membrane vascular density in alligator but not chicken embryos. Comp. Biochem. Physiol. A Mol. Integr. Physiol. 125, 57–61.

Crivellato, E., 2011. The role of angiogenic growth factors in organogenesis. Int. J. Dev. Biol. 55, 365–375.

de Meer, K., Heymans, H.S., Zijlstra, W.G., 1995. Physical adaptation of children to life at high altitude. Eur. J. Pediatr. 154, 263–272.

Druyan, S., Levi, E., 2012. Reduced O_2 concentration during CAM development—its effect on angiogenesis and gene expression in the broiler embryo CAM. Gene Expr. Patterns 12, 236–244.

Duncker, H.R., 1971. The lung–air sac system of birds. A contribution to the functional anatomy of the respiratory apparatus. Ergeb. Anat. Entwicklungsgesch. 45, 1–171.

Duncker, H.R., 2004. Vertebrate lungs: structure, topography and mechanics. A comparative perspective of the progressive integration of respiratory system, locomotor apparatus and ontogenetic development. Respir. Physiol. Neurobiol. 144, 111–124.

Dzialowski, E.M., von Plettenberg, D., Elmonoufy, N.A., Burggren, W.W., 2002. Chronic hypoxia alters the physiological and morphological trajectories of developing chicken embryos. Comp. Biochem. Physiol. A Mol. Integr. Physiol. 131, 713–724.

Fujinaga, H., Baker, C.D., Ryan, S.L., Markham, N.E., Seedorf, G.J., Balasubramaniam, V., Abman, S.H., 2009. Hyperoxia disrupts vascular endothelial growth factor-nitric oxide signaling and decreases growth of endothelial colony-forming cells from preterm infants. Am. J. Physiol. Lung Cell. Mol. Physiol. 297, L1160–L1169.

Garcia, A.M., Ladage, M.L., Dumesnil, D.R., Zaman, K., Shulaev, V., Azad, R.K., Padilla, P.A., 2015. Glucose induces sensitivity to oxygen deprivation and modulates insulin/IGF-1 signaling and lipid biosynthesis in Caenorhabditis elegans. Genetics 115, 174631.

Gebb, S.A., Jones, P.L., 2003. Hypoxia and lung branching morphogenesis. Adv. Exp. Med. Biol. 543, 117–125.

Gorr, T.A., Wichmann, D., Hu, J., Hermes-Lima, M., Welker, A.F., Terwilliger, N., Wren, J.F., Viney, M., Morris, S., Nilsson, G.E., Deten, A., Soliz, J., Gassmann, M., 2010. Hypoxia tolerance in animals: biology and application. Physiol. Biochem. Zool. 83, 733–752.

Hamburger, V., Hamilton, H.L., 1951. A series of normal stages in the development of the chick embryo. J. Morphol. 88, 49–92.

Haworth, S.G., Hislop, A.A., 2003. Lung development-the effects of chronic hypoxia. Semin. Neonatol. 8, 1–8.

Hines, E.A., Sun, X., 2014. Tissue crosstalk in lung development. J. Cell. Biochem. 115, 1469–1477.

Hislop, A., 2005. Developmental biology of the pulmonary circulation. Paediatr. Respir. Rev. 6, 35–43.

Keenaghan, M., Cai, C.L., Kumar, D., Valencia, G.B., Rao, M., Aranda, J.V., Beharry, K.D., 2013. Response of vascular endothelial growth factor and

angiogenesis-related genes to stepwise increases in inspired oxygen in neonatal rat lungs. Pediatr. Res. 73, 630–638.
Kumar, V.H., Ryan, R.M., 2004. Growth factors in the fetal and neonatal lung. Front. Biosci. 9, 464–480.
Lazarus, A., Keshet, E., 2011. Vascular endothelial growth factor and vascular homeostasis. Proc. Am. Thorac. Soc. 8, 508–511.
Maina, J.N., 2002a. Fundamental structural aspects and features in the bioengineering of the gas exchangers: comparative perspectives. Adv. Anat. Embryol. Cell. Biol. 163 (III–XII), 1–108.
Maina, J.N., 2002b. Some recent advances on the study and understanding of the functional design of the avian lung: morphological and morphometric perspectives. Biol. Rev. 77, 97–152.
Maina, J.N., 2003a. Developmental dynamics of the bronchial (airway) and air sac systems of the avian respiratory system from day 3 to day 26 of life: a scanning electron microscopic study of the domestic fowl, *Gallus gallus* variant domesticus. Anat. Embryol. 207, 119–134.
Maina, J.N., 2003b. A systematic study of the development of the airway (bronchial) system of the avian lung from days 3 to 26 of embryogenesis: a transmission electron microscopic study on the domestic fowl, *Gallus gallus* variant domesticus. Tissue Cell 35, 375–391.
Maina, J.N., 2005. The Lung Air Sac System of Birds: Development, Structure, and Function. Springer-Verlag, Heidelberg.
Maina, J.N., 2006. Development, structure, and function of a novel respiratory organ, the lung–air sac system of birds: to go where no other vertebrate has gone. Biol. Rev. Camb. Philos. Soc. 81, 545–579.
Maina, J.N., 2015. Structural and biomechanical properties of the exchange tissue of the avian lung. Anat. Rec., http://dx.doi.org/10.1002/ar.23162 (epub ahead of print).
Maina, J.N., King, A.S., Settle, G., 1989. An allometric study of pulmonary morphometric parameters in birds, with mammalian comparisons. Philos. Trans. R. Soc. Lond. B Biol. Sci. 326, 1–57.
Maina, J.N., West, J.B., Orgeig, S., Foot, N.J., Daniels, C.B., Kiama, S.G., Gehr, P., Muhlfeld, C., Blank, F., Muller, L., Lehmann, A., Brandenberger, C., Rothen-Rutishauser, B., 2010. Recent advances into understanding some aspects of the structure and function of mammalian and avian lungs. Physiol. Biochem. Zool. 83, 792–807.
Maina, J.N., Woodward, J.D., 2009. Three-dimensional serial section computer reconstruction of the arrangement of the structural components of the parabronchus of the Ostrich, *Struthio camelus* lung. Anat. Rec. 292, 1685–1698.
Makanya, A., Anagnostopoulou, A., Djonov, V., 2013. Development and remodeling of the vertebrate blood-gas barrier. BioMed. Res. Int. 2013, 101597.
Makanya, A.N., Djonov, V., 2009. Parabronchial angioarchitecture in developing and adult chickens. J. Appl. Physiol. 106, 1959–1969.
Makanya, A.N., El-Darawish, Y., Kavoi, B.M., Djonov, V., 2011a. Spatial and functional relationships between air conduits and blood capillaries in the pulmonary gas exchange tissue of adult and developing chickens. Microsc. Res. Tech. 74, 159–169.
Makanya, A.N., Hlushchuk, R., Djonov, V., 2011b. The pulmonary blood-gas barrier in the avian embryo: inauguration, development and refinement. Respir. Physiol. Neurobiol. 178, 30–38.
Maniscalco, W.M., Watkins, R.H., D'Angio, C.T., Ryan, R.M., 1997. Hyperoxic injury decreases alveolar epithelial cell expression of vascular endothelial growth factor (VEGF) in neonatal rabbit lung. Am. J. Respir. Cell Mol. Biol. 16, 557–567.
Molenaar, R., van den Anker, I., Meijerhof, R., Kemp, B., van den Brand, H., 2011. Effect of eggshell temperature and oxygen concentration during incubation on the developmental and physiological status of broiler hatchlings in the perinatal period. Poult. Sci. 90, 1257–1266.
Mortola, J.P., 2009. Gas exchange in avian embryos and hatchlings. Comp. Biochem. Physiol. A Mol. Integr. Physiol. 153, 359–377.
Mueller, C.A., Burggren, W., Tazawa, H., 2015. The physiology of the avian embryo. In: Whittow, G.C. (Ed.), Sturkie's Avian Physiology. , 6th ed. Elsivier, New York.
Padmanabha, D., Padilla, P.A., You, Y.J., Baker, K.D., 2015. A HIF-Independent mediator of transcriptional responses to oxygen deprivation in *Caenorhabditis elegans*. Genetics 199, 739–748.
Prabhakar, N.R., Semenza, G.L., 2012. Adaptive and maladaptive cardiorespiratory responses to continuous and intermittent hypoxia mediated by hypoxia-inducible factors 1 and 2. Physiol. Rev. 92, 967–1003.
Remesal, A., Pedraz, C., San Feliciano, L., Ludena, D., 2009. Pulmonary expression of vascular endothelial growth factor (VEGF) and alveolar septation in a newborn rat model exposed to acute hypoxia and recovered under conditions of air or hyperoxia. Histol. Histopathol. 24, 325–330.
Romanoff, A.L., 1960. The Avian Embryo: Structural and Functional Development. Macmillan, New York.
Scheid, P., 1979. Mechanisms of gas exchange in bird lungs. Rev. Physiol. Biochem. Pharmacol. 86, 137–186.
Shenberger, J.S., Zhang, L., Powell, R.J., Barchowsky, A., 2007. Hyperoxia enhances VEGF release from A549 cells via post-transcriptional processes. Free Radic. Biol. Med. 43, 844–852.
Stock, M.K., Metcalfe, J., 1987. Modulation of growth and metabolism of the chick embryo by a brief (72-hr) change in oxygen availability. J. Exp. Zool. Suppl. 1, 351–356.
Strick, D.M., Waycaster, R.L., Montani, J.P., Gay, W.J., Adair, T.H., 1991. Morphometric measurements of chorioallantoic membrane vascularity: effects of hypoxia and hyperoxia. Am. J. Physiol. 260, H1385–1389.
Symonds, M.E., Stephenson, T., Gardner, D.S., Budge, H., 2007. Long-term effects of nutritional programming of the embryo and fetus: mechanisms and critical windows. Reprod. Fertil. Dev. 19, 53–63.
Taylor, C.T., McElwain, J.C., 2010. Ancient atmospheres and the evolution of oxygen sensing via the hypoxia-inducible factor in metazoans. Physiology 25, 272–279.
Tazawa, H., 1981. Adverse effect of failure to turn the avian egg on the embryo oxygen exchange. Respir. Physiol. 41, 137–142.
Tuder, R.M., Yun, J.H., Bhunia, A., Fijalkowska, I., 2007. Hypoxia and chronic lung disease. J. Mol. Med. 85, 1317–1324.
Tzaneva, V., Bailey, S., Perry, S.F., 2011. The interactive effects of hypoxemia, hyperoxia, and temperature on the gill morphology of goldfish (*Carassius auratus*). Am. J. Physiol. Regul. Integr. Comp. Physiol. 300, R1344–R1351.
van Patot, M.C., Gassmann, M., 2011. Hypoxia: adapting to high altitude by mutating EPAS-1, the gene encoding HIF-2alpha. High Alt. Med. Biol. 12, 157–167.
Voelkel, N.F., Vandivier, R.W., Tuder, R.M., 2006. Vascular endothelial growth factor in the lung. Am. J. Physiol. Lung. Cell. Mol. Physiol. 290, L209–L221.
Wang, L., Shi, P., Xu, Z., Li, J., Xie, Y., Mitton, K., Drenser, K., Yan, Q., 2014. Up-regulation of VEGF by retinoic acid during hyperoxia prevents retinal neovascularization and retinopathy. Invest. Ophthalmol. Vis. Sci. 55, 4276–4287.
West, J.B., 2009. Comparative physiology of the pulmonary blood-gas barrier: the unique avian solution. Am. J. Physiol. Regul. Integr. Comp. Physiol. 297, R1625–R1634.
West, J.B., 2011. Comparative physiology of the pulmonary circulation. Compr. Physiol. 1, 1525–1539.
Whittow, G.C., 2015. Sturkie's Avian Physiology. In: Whittow, G.C. (Ed.), 6th ed. Elsivier, New York.
Woik, N., Kroll, J., 2015. Regulation of lung development and regeneration by the vascular system. Cell. Mol. Life Sci. 72 (14), 2709–2718.
Woodward, J.D., Maina, J.N., 2005. A 3D digital reconstruction of the components of the gas exchange tissue of the lung of the muscovy duck, *Cairina moschata*. J. Anat. 206, 477–492.
Woodward, J.D., Maina, J.N., 2008. Study of the structure of the air and blood capillaries of the gas exchange tissue of the avian lung by serial section three-dimensional reconstruction. J. Microsc. 230, 84–93.
Wu, S.C., Zhang, Y., 2010. Active DNA demethylation: many roads lead to Rome. Nat. Rev. Mol. Cell Biol. 11, 607–620.
Xiao, W., 2015. The hypoxia signaling pathway and hypoxic adaptation in fishes. Sci. China Life Sci. 58, 148–155.
Xu, L.J., Mortola, J.P., 1989. Effects of hypoxia or hyperoxia on the lung of the chick embryo. Can. J. Physiol. Pharmacol. 67, 515–519.
Zhang, H., Burggren, W.W., 2012. Hypoxic level and duration differentially affect embryonic organ system development of the chicken (*Gallus gallus*). Poult. Sci. 91, 3191–3201.